Implications for Differential Diagnosis of Lung Cancer–Associated Lymphadenopathy in Lymphoepithelioid Cell Lymphoma (Lennert's Lymphoma) Arising Simultaneously with Lung Cancer

A Case Report

Rira Hoshi, C.T., C.I.A.C., **Noriyuki Furuta,** C.T., C.M.I.A.C., **Takeshi Horai,** M.D., M.I.A.C., **Kengo Takeuchi,** M.D., **Yuichi Ishikawa,** M.D., and **Yukitoshi Satoh,** M.D., F.I.A.C.

Background

Lymphoepithelioid cell lymphoma (LCL) is a rare morphologic variant of peripheral T-cell lymphoma, and its cytologic features have not been well characterized. We describe details from fine needle aspiration cytology (FNAC) of LCL in a patient simultaneously suffering from lung cancer, in whom extensive lymph node metastasis was suspected clinically.

Case

A 54-year-old man had a lung nodule diagnosed as an adenocarcinoma by biopsy. 18F-fluoro-deoxyglucose positron emission tomography showed high uptake in the lung nodule as well as interlobar, supraclavicular and axillary lymph nodes. FNAC from interlobar and supraclavicular lymph nodes revealed abundant lymphoid cells intermingled with epithelioid cell clusters. Most lymphoid cells were small, with teardrop-shaped nuclei. Occasionally, large lymphoid cells with hyperconvoluted nuclei and prominent nucleoli were observed. An extensive sarcoid reaction was suspected on cytology, and lobectomy was performed. LCL with lung adenocarcinoma was diagnosed on the immunohistochemical findings.

Conclusion

Detailed observation of lymphoid cells with FNAC is important even in patients with lung cancer and massive regional lymphadenopathy. Presence of a teardrop nuclear shape and nuclear irregularities of lymphoid cells provides important information for cytologic diagnosis of LCL when epithelioid cell clusters are evident. (Acta Cytol 2010;54:197–201)

It is important to carefully examine the morphology of lymphoid cells on FNAC even if metastasis from a malignant tumor such as lung cancer is highly suspected.

Keywords: aspiration cytology, fine-needle; lung cancer; lymph node metastasis; lymphoepithelioid cell lymphoma; sarcoid reaction.

Lymphoepithelioid cell lymphoma (LCL) considered to be a rare variant of peripheral T-cell lymphoma, unspecified, in the World Health Organization (WHO) classification.[1,2] Its major cytologic feature is the presence of epithelioid cell clusters intermingled with atypical lymphoid cells.[3–17] Although several case reports of LCL have appeared in the literature, detailed cytologic features have yet to be established.[11–17]

The frequency of synchronous nodal lymphomas and lung cancer is in the range of 0.13% to ~0.43% of all lung cancers in Japan.[18] To our knowledge, however, simultaneous LCL with lung cancer has never been reported. Many nodal lesions seen in patients with lung cancer are sarcoid reactions and nodal reactive changes, including granulomatous lymphadenitis,[13,19] and need to be distin-

From the Departments of Cytology and Pathology, Cancer Institute Hospital, Japanese Foundation for Cancer Research, Tokyo; and Department of Thoracic Surgery, Kitasato University School of Medicine, Kanagawa, Japan.

Ms. Hoshi is Cytotechnologist, Department of Cytology, Cancer Institute Hospital, Japanese Foundation for Cancer Research.

Mr. Furuta is Chief, Department of Cytology, Cancer Institute Hospital, Japanese Foundation for Cancer Research.

Dr. Horai is Cytopathologist, Department of Cytology, Cancer Institute Hospital, Japanese Foundation for Cancer Research.

Dr. Takeuchi is Staff Scientist, Department of Pathology, Cancer Institute Hospital, Japanese Foundation for Cancer Research.

Dr. Ishikawa is Chief, Department of Pathology, Cancer Institute Hospital, Japanese Foundation for Cancer Research.

Dr. Satoh is Professor, Department of Thoracic Surgery, Kitasato University School of Medicine.

Supported by grants-in-aid from the Ministry of Education, Sports, Culture, Science and Technology and grants from the Ministry of Health, Labour and Welfare, the Smoking Research Foundation and the Vehicle Racing Commemorative Foundation.

Address correspondence to: Yukitoshi Satoh, M.D., F.I.A.C., Department of Thoracic Surgery, Kitasato University School of Medicine, 1-15-1 Kitasato, Sagamihara-shi, Kanagawa 228-8555, Japan (ysatoh@med.kitasato-u.ac.jp).

Financial Disclosure: The authors have no connection to any companies or products mentioned in this article.

Received for publication December 7, 2007.

Accepted for publication February 2, 2008.

guished from LCL cytologically.[3-17]

We describe a rare case of simultaneous LCL with lung cancer. Extensive lymph node metastasis was suspected on imaging, but a sarcoid reaction was indicated by fine needle aspiration cytology (FNAC). We discuss cytologic pitfalls and detailed characteristics of LCL.

Case Report

A 54-year-old Japanese man was referred to our hospital for further examination of a right lung nodule found on chest radiography at a regular health check-up. Chest computed tomography (CT) showed a 24-mm nodule with spiculation and pleural indentation in the right upper lung field and lymphadenopathy involving the mediastinal, subcarinal, interlobar and left axillary lymph nodes. Transbronchial FNA (TBAC) and biopsy from the nodule revealed a primary lung adenocarcinoma. FNAC from interlobar and subcarinal lymph nodes was then performed for diagnosis of the apparent metastasis. Cytology for interlobar lymph nodes revealed a few atypical cells, but no unequivocal malignancy. Whole-body positron emission tomography revealed increased 18F-fluoro-deoxyglucose uptake in the right lung nodule and interlobar, right supraclavicular and left axillary lymph nodes; FNAC and biopsy of a supraclavicular lymph node were performed. This revealed atypical lymphoid cells, again with uncertainty as to whether they were malignant or reactive in nature. Examination of biopsy material from interlobar, subcarinal and supraclavicular lymph nodes resulted in a diagnosis of sarcoid reactions in all cases.

The presence of teardrop-shaped nuclei and nuclear irregularity of small lymphoid cells admixed with epithelioid cell clusters could be helpful for cytologic diagnosis of LCL.

With the clinical diagnosis of stage I disease, the patient underwent right upper lobectomy with mediastinal lymph node dissection. The interlobar lymph node was diagnosed as demonstrating granulomatous lymphadenitis from examination of intraoperative frozen sections. Finally, the pulmonary nodule was diagnosed as a stage I poorly differentiated adenocarcinoma. Based on further immunohistochemical studies, the interlobar lymph node was diagnosed as LCL. Thus we reviewed the biopsy material obtained from a supraclavicular lymph node and added immunohistochemical investigation. The final diagnosis was LCL. As a result of 6 cycles of chemotherapy with Adriamycin, cyclophosphamide, vincristine and prednisone, he is now in complete remission after 10 months of follow-up. Unfortunately, he had lung cancer recurrence locoregionally 2 years after the surgery, but is now alive after 3 years of follow-up.

Right Upper Lobe Lung Cancer

Cytologic Findings. The smears of TBAC were moderately cellular, with cohesive clusters of large tumor cells on a necrotic background (Figure 1). The tumor cells were polygonal to cuboidal, with abundant homogenously staining cytoplasm, hyperconvoluted nuclei with a finely reticular chromatin pattern, thickened nuclear membranes and a single to several and prominent nucleoli. There was no evidence of glandular structures.

Histopathologic Findings. Grossly, the resected pulmonary tumor was a solid, gray-white, firm nodule, 21 mm in diameter, located in the peripheral portion of the right upper lobe. Microscopically, the tumor consisted of sheets of large polygonal cells with occasional mucin vacuoles (Figure 2). The tumor cells had hyperconvoluted nuclei, and markedly cellular pleomorphism was evident. Papillary structures were observed within the lesion focally.

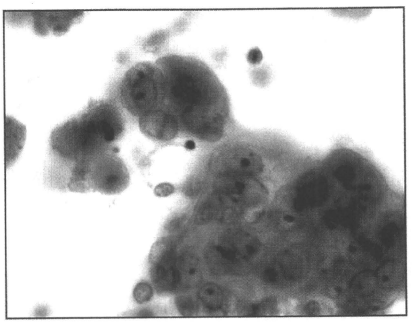

Figure 1 TBAC smear from the lung cancer. The cohesive clusters of polygonal to cuboidal tumor cells (Papanicolaou stain, ×1,000).

Lymphoepithelioid Cell Lymphoma

Cytologic Findings. The smears of TBAC from an interlobar lymph node and FNAC from a supraclavicular lymph node were highly cellular, with numerous lymphoid cells and occasional dispersed epithelioid cell clusters (Figure 3). Most of the lymphoid cells were small, with frequent teardrop-shaped nuclei (Figure 4). Occasionally, isolated and large lymphoid cells were evident (Figure 5) with a round shape and pale or clear cytoplasm. These cells had hyperconvoluted nuclei with a finely granular chromatin pattern and thin nuclear membranes. Single to several large, round to irregularly shaped nucleoli were seen.

The epithelioid cell clusters consisted of small, monolayered and loose aggregates of 10–20 spindle cells with abundant, pale-staining

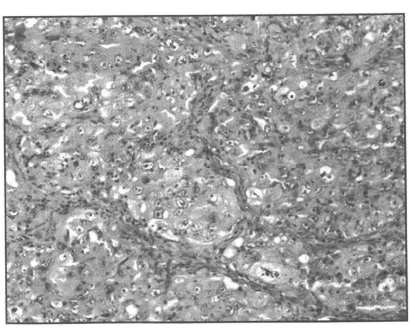

Figure 2 Histologic findings of the resected lung cancer. Sheets of large and polygonal cells with marked cellular pleomorphism (hematoxylin-eosin, ×200).

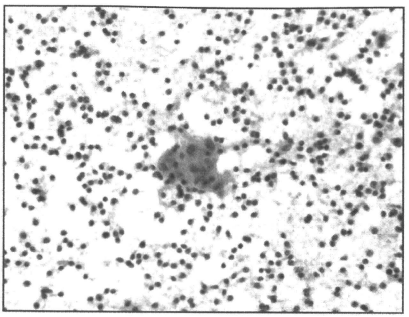

Figure 3 TBAC smear of LCL. The cohesive clusters of epithelioid cells with many atypical lymphoid cells (Papanicolaou stain, ×400).

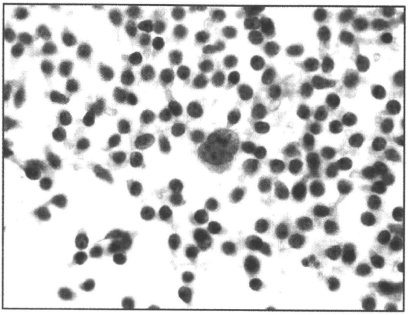

Figure 5 TBAC smear of LCL. Occasional atypical large lymphoid cells with hyperconvoluted nuclei and prominent nucleoli (Papanicolaou stain, × 1,000).

and homogeneous cytoplasm. Oval to elongated nuclei with single small nucleoli were evident.

Histopathologic Findings. Dissected interlobar, hilar and mediastinal lymph nodes were all enlarged. Microscopically, nodal structures in the obtained materials were precluded by the presence of epithelioid histiocytes usually grouped in small clusters (Figure 6A). The lymphoid component was heterogeneous in population, including small and medium-sized to large cells, eosinophils and plasma cells. Most of the lymphoid cells had irregularly shaped nuclei, granular chromatin and prominent nucleoli. Occasionally, large cells resembling Reed-Sternberg cells were observed. Immunohistochemical studies of the lymph nodes were performed with a labeled streptavidin-biotin staining kit (Dako, Carpinteria, California, U.S.A.) according to the manufacturer's instructions. The results were classified as follows: negative—the absence of positive-stained tumor cells; weakly positive—the presence of tumor cells expressing the antigen more weakly than normal T-cells of positive controls; and positive—the presence of tumor cells expressing the antigen as strongly as normal T-cells of positive controls. Immunohistochemically, the lymphoid cells were positive for CD8 (Nichirei, Tokyo, Japan) (Figure 6B) and weakly positive for CD3 (Dako, Glostrup, Denmark), CD7 (Novocastra, Newcastle upon Tyne, U.K.) and CD30 (Dako). Immunostaining for CD4 (Nichirei), CD5 (Novocastra), CD15 (Becton-Dickinson, Mountain View, California, U.S.A.), CD20 (Dako), perforin (Novocastra) and Granzyme B (Dako) was negative (Table I). These findings indicate a T-cell lineage. Because large cells resembling Reed-Sternberg cells showed positivity for CD8, as did small and medium-sized lymphoid cells, Hodgkin's disease was excluded. In situ hybridization using a fluorescein-conjugated oligonucleotide probe for Epstein-Barr virus–encoded RNA was performed with paraffin-embedded specimens.[20,21] As a result, the Epstein-Barr virus–encoded RNA probe detected no evident Epstein-Barr virus infection. The histologic features of biopsy material obtained from a supraclavicular lymph node were similar to those described earlier. Finally, these lymph nodes were diagnosed as LCL by the WHO classification.[1]

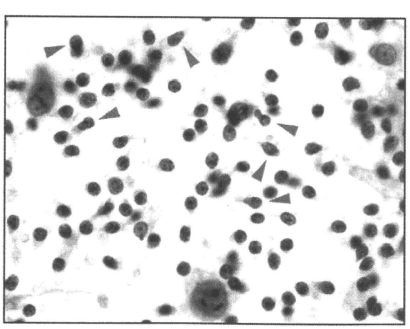

Figure 4 TBAC smear of LCL. Atypical small lymphoid cells with teardrop-shaped nuclei (arrowheads) (Papanicolaou stain, × 1,000).

Discussion

Complete and accurate mediastinal staging of patients with lung cancer is essential for determining prognosis and guiding optimal treatment strategies. Therefore, for patients with lung cancer accompanied by lymphadenopathy, it is important to indicate whether the cause of the lymphadenopathy is metastasis. For differential diagnosis of lymphadenopathy in patients with lung cancer, several reports have indicated that sarcoid reactions require particular attention in this regard.[22,23] For staging lung cancer, FNAC has demonstrated a sensitivity of 76.0–95.7%, a specificity of 100% and a diagnostic accuracy of 98.0%, with fewer false positive results than with CT and PET.[24,25] In our case, because extensive lymphadenopathy was apparent, FNAC was performed and a sarcoid reaction was diagnosed cytologically. On pathologic examination and immunohistochemical analysis of resected materials, however, lymph nodes were diagnosed as LCL.

LCL is now included in the category of peripheral T-cell lymphomas, unspecified, by the WHO classification.[1] Atypical lymphoid cells express variable T-lineage markers, such as CD2, CD3, CD4, CD5, CD7, CD8, CD43 and CD45RO, and lack expression of B-lineage markers.[9-17,26,27] Previously the immunocytochemical characteristics of LCL cells were thought to be CD4-positive and CD8-negative. In some cases of LCL, however, the neoplastic cells were CD8-positive and CD4-negative, a well-known variant of LCL.[28] Moreover, Epstein-Barr virus infection is occasionally

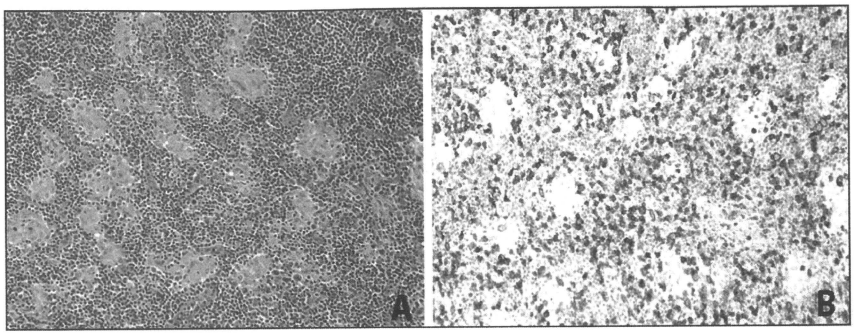

Figure 6 Histologic findings of LCL. (A) Aggregates of epithelioid cells interspersed between atypical lymphoid cells. (B) Immunoreactivity of lymphoid cells for CD8 (A, hematoxylin-eosin, ×200; B, immunostain, ×200).

demonstrated in reactive bystander B cells in LCL and is thought to be associated with a poor prognosis.[28] LCL patients usually present with generalized disease, often involving systemic lymph nodes.[29] In spite of morphologic features mimicking granulomatous disease, LCL is considered to show aggressive behavior clinicopathologically.[26,29] Therefore it is important to alert the clinician to the possibility of this disease.

Although several cytologic reports of LCL have appeared in the literature, simultaneous LCL with lung cancer has not described. Cytologic materials obtained from lymph nodes of our case included a lymphoid population consisting of a few large cells intermingled with numerous small cells. Moreover, these large lymphoid cells had hyperconvoluted nuclei and prominent nucleoli, raising the possibility of metastasis from co-present lung cancer. Cytologic discrimination of the large lymphoid cells was facilitated by the following characteristics: absence of adhesive clusters, round shape, scant and clear cytoplasm with distinct cell borders, round nuclei with thin nuclear membranes and finely granular and homogeneous nuclear chromatin. In spite of these distinctive features, however, we could not diagnose initially LCL in this case because of concern regarding the possibility of metastasis.

Review of the literature[11-17] shows the presence of atypical lymphoid cells with irregular nuclei to be a cytologic feature of non-Hodgkin's lymphoma (NHL), including LCL, on FNAC. As confirmed by the present case, it is important for cytologic diagnosis to focus on nuclear irregularity. In addition, the nuclei of small lymphoid cells frequently showed a teardrop shape in the smears of our case. To our knowledge, teardrop-shaped nuclei are rarely seen in smears obtained from normal lymph nodes or benign lesions such as granulomatous lymphadenitis. Therefore this feature may be of assistance for cytologic diagnosis of NHL, including LCL. Because many cases of NHL present as homogeneous populations of medium to large lymphocytes,[11-16,27] the finding of heterogeneity may point to an LCL.

In earlier cytology reports, the presence of epithelioid cell clusters showing small, monolayered and loose aggregates of spindle cells was a major feature on FNAC of LCL.[11-17] They were also present in our case. However, the existence of epithelioid cell clusters may in fact be a pitfall for cytologic diagnosis, because such clusters are also featured in sarcoid reactions.[13,30,31]

Several reports have indicated that Hodgkin's disease needs to be differentiated from LCL.[13,14,17] In the present case, the finding that atypical large lymphoid cells were smaller than Reed-Sternberg cells, together with the teardrop-shaped nuclei and binuclei, made for a clear diagnosis.

In conclusion, it is important to carefully examine the morphology of lymphoid cells on FNAC even if metastasis from a malignant tumor such as lung cancer is highly suspected. The presence of teardrop-shaped nuclei and nuclear irregularity of small lymphoid cells admixed with epithelioid cell clusters could be helpful for cytologic diagnosis of LCL.

Table I *Immunohistochemical Findings*

Primary antibodies	Source	Results
CD3	Dako	Weakly +
CD4	Nichirei	–
CD5	Novocastra	–
CD7	Novocastra	Weakly +
CD8	Nichirei	+
CD15	Becton-Dickinson	–
CD20	Dako	–
CD30	Dako	Weakly +
Perforin	Novocastra	–
Granzyme B	Dako	–

+ = Tumor cells expressed the antigen as strongly as normal T-cells of positive controls, weakly + = the tumor cells expressed the antigen more weakly than normal T-cells of positive controls.

Acknowledgments

We thank Mr. Masafumi Tsuzuku and Dr. Yasuo Hirai for their advice with cytology; Mss. Tomoko Kakita, Reimi Asaka and Kazuko Yokokawa for their technical expertise; and Drs. Ken Nakagawa and Sakae Okumura for their clinical assistance.

References

1. Ralfkiaer E, Müller-Hermelink HK, Jaffe ES: Peripheral T-cell lymphoma, unspecified. *In* World Health Organization Classification of Tumours: Pathology and Genetics of Tumours of Hematopoietic and Lymphoid Tissues: Lyon, IARC Press, 2001, pp 227–229
2. Rüdiger T, Weisenburger DD, Anderson JR, Armitage JO, Diebold J, MacLennan KA, Nathwani BN, Ullrich F, Müller-Hermelink HK; Non-Hodgkin's Lymphoma Classification Project: Peripheral T-cell lympho-

ma (excluding anaplastic large-cell lymphoma): Results from the Non-Hodgkin's Lymphoma Classification Project. Ann Oncol 2002;13:140–149

3. Lennert K, Mestdagh J: Lymphogranulomatosen mit konstant hohem Epithelioidzellgehalt. Virchows Arch (A) 1968;344:1–20
4. Burke JS, Butler JJ: Malignant lymphoma with a high content of epithelioid histiocytes (Lennert's lymphoma). Am J Clin Pathol 1976;66:1–9
5. Klein MA, Jaffe R, Neiman RS: Lennert's lymphoma with transformation to malignant lymphoma, histiocytic type. Am J Pathol 1977;68:601–605
6. Kim H, Jacobs C, Warnke RA, Dorfman RF: Malignant lymphoma with a high content of epithelioid histiocytes: A distinct clinicopathologic entity and a form of so-called "Lennert's lymphoma." Cancer 1978;41: 620–635
7. Palutke M, Varadachari C, Weise RW, Husain M, Tabazka P: Lennert's lymphoma, a T-cell neoplasm. Am J Clin Pathol 1978;69:643–646
8. Warnke RA, Weiss LM, Chan JK, Cleary ML, Dorfman RF: Tumors of the lymph nodes and spleen. *In* Atlas of Tumor Pathology. Third series. Washington, DC, Armed Forces Institute of Pathology, 1995, pp 259–276
9. Patsouris E, Noël H, Lennert K: Histological and immunohistological findings in lymphoepithelioid cell lymphoma (Lennert's lymphoma). Am J Surg Pathol 1988;12:341–350
10. Pinkus GS, O'Hara CJ, Said JW: Peripheral/post-thymic T-cell lymphomas: A spectrum of disease: Clinical, pathologic and immunologic features of 78 cases. Cancer 1990;65:971–998
11. Park A, Kim CW: FNAC of malignant lymphoma in an area with a high incidence of T-cell lymphoma: Correlation of accuracy of cytologic diagnosis with histologic subtype and immunophenotype. Acta Cytol 1999; 43:1059–1069
12. Oertel J, Oertel B, Lobeck H, Huhn D: Cytologic and immunocytologic studies of peripheral T-cell lymphomas. Acta Cytol 1991;35:285–293
13. Gray W: Lymph nodes and other lymphoreticular organs. *In* Diagnostic Cytopathology. Second edition, Edinburgh, Churchill Livingstone, 2003, pp 501–547
14. Vaillo Viragre A, Gutierrez Martin A, Perez Barrios A, Alberti Masgrau N, Ruiz Liso JM: Lymphoepithelioid cell lymphoma (Lennert's lymphoma): Report of a case with fine needle aspiration cytology. Acta Cytol 2004;48:234–238
15. Katz RL, Grinstman A, Cabanillas F, Fanning CV, Dekmezian RH, Ordonez NG, Balogie B, Butler JJ: Fine needle aspiration cytology of peripheral T-cell lymphoma: A cytologic, immunologic and cytometric study. Am J Clin Pathol 1989;19:120–131
16. Sneige N, Dekmezian RH, Katz RL, Fanning TV, Lukeman JL, Ordoñez NF, Cabanillas FF: Morphologic and immunocytochemical evaluation of 220 fine needle aspirates of malignant lymphoma and lymphoid hyperplasia. Acta Cytol 1990;34:311–322
17. Daneshbod Y: Cytologic findings of peripheral T-cell lymphoma (PTCL) with high epithelioid cell content (Lennert's lymphoma) in imprint smear: A case report. CytoJournal 2006;3:3 (epub)
18. Machinami R: Annual of the Pathological Autopsy Cases in Japan. Edited by the Japanese Society of Pathology. Tokyo, JSP 1998;41:1190–1199
19. Gorton G, Linell F: Malignant tumours and sarcoid reactions in regional lymph nodes. Acta Radiol 1957;47:381–392
20. Barletta JM, Kingma DW, Ling Y, Charache P, Mann RB, Ambinder RF: Rapid in situ hybridization for the diagnosis of latent Epstein-Barr virus infection. Mol Cell Probes 1993;7:105–109
21. Fan H, Gulley ML: Molecular methods for detecting Epstein-Barr virus. *In* Molecular Pathology Protocols. Edited by Killeen AA. Totowa, NJ, Humana Press, 2001, pp 301–312
22. Lowe VJ, Naunheim KS: Positron emission tomography in lung cancer. Ann Thorac Surg 1998;65:1821–1829
23. Maeda J, Ohta M, Hirabayashi H, Masuda H: False positive accumulation in 18F-fluorodeoxyglucose positron emission tomography scan due to sarcoid reaction following induction chemotherapy for lung cancer. Jpn J Thorac Cardiovasc Surg 2005;53:196–198
24. Gasparini S: Evolving role of interventional pulmonology in the interdisciplinary approach to the staging and management of lung cancer: Bronchoscopic mediastinal staging of lung cancer. Clin Lung Cancer 2006;8:110–115
25. Yasufuku K, Nakajima T, Motoori K, Sekine Y, Shibuya K, Hiroshima K, Fujisawa T: Comparison of endobronchial ultrasound, positron emission tomography, and CT for lymph node staging of lung cancer. 2006;130:710–718
26. Ralfkiaer E, Müller-Hermelink HK, Jaffe ES: Peripheral T-cell lymphoma, unspecified. *In* Pathology and Genetics of Tumours of Haematopoietic and Lymphoid Tissues. Edited by ES Jaffe, NL Harris, H Stein, JW Vardiman. Lyon, IARC Press, 2001
27. Al Shanqeety O, Mourad WA: Diagnosis of peripheral T-cell lymphoma by fine-needle aspiration biopsy: A cytomorphologic and immunophenotypic approach. Diagn Cytopathol 2000;23:375–379
28. Yamashita Y, Nakamura S, Kagami Y, Hasegawa Y, Kojima H, Nagasawa T, Mori N: Lennert's lymphoma: A variant of cytotoxic T-cell lymphoma? Am J Surg Pathol 2000;24:1627–1633
29. Spier CM, Lippmann SM, Miller TP, Grogan TM: Lennert's lymphoma: A clinicopathologic study with emphasis on phenotype and its relationship to survival. Cancer 1988;61:517–524
30. Frischer-Ravens A, Sriram PV, Topalidis T, Hauber HP, Meyer A, Soehendra N, Pforte A: Diagnosing sarcoidosis using endosonography-guided fine needle aspiration. Chest 2000;118:928–935
31. Viguer JM, Jimenez-Heffernan JA, Lopez-Ferrer P, Gonzalez-Peramato P, Vicandi B: Fine needle aspiration of toxoplasmic (Piringer-Kuchinka) lymphadenitis: A cytohistologic correlation study. Acta Cytol 2005;49: 139–143

Cancer Science
The official journal of the Japanese Cancer Association

Sensitive immunohistochemical detection of WT1 protein in tumors with anti-WT1 antibody against WT1 235 peptide

Ryo Ichinohasama,[1,8] Yusuke Oji,[2] Hisayuki Yokoyama,[3] Kengo Takeuchi,[4] Tohru Fujiwara,[3] Kenichi Ishizawa,[1,3] Osamu Taniguchi,[5] Akihiro Tsuboi,[6] Yoshihiro Oka[6,7] and Haruo Sugiyama[5]

[1]Division of Hematopathology, Tohoku University Graduate School of Medicine, Sendai; [2]Department of Bioinformatics, Osaka University Graduate School of Medicine, Osaka; [3]Department of Hematology and Rheumatology, Tohoku University Graduate School of Medicine, Sendai; [4]Department of Pathology, Cancer Institute, Japanese Foundation for Cancer Research, Tokyo; Departments of [5]Functional Diagnostic Science, [6]Cancer Immunotherapy, [7]Respiratory Medicine, Allergy and Rheumatic Diseases, Osaka University Graduate School of Medicine, Osaka, Japan

(Received December 11, 2009/Revised January 25, 2010/Accepted January 27, 2010/Online publication February 22, 2010)

The Wilms' tumor 1 (WT1) gene is overexpressed in leukemia and various types of solid tumor, such as lung and colorectal cancer, and plays an oncogenic role in their tumorigenesis. Recent studies have demonstrated the potential of WT1-targeting cancer immunotherapy in clinical settings. As expression of WT1 protein in tumor cells is a prerequisite for WT1-targeting immunotherapy, immunohistochemical methods to detect WT1 protein with high sensitivity and specificity are required. In the present study, we developed a rabbit polyclonal antibody (WT1-R) against the 9-mer WT1 235 peptide, which is used for vaccination. The specificity of WT1-R was confirmed by immunoprecipitation, western blotting analysis, and competitive enzyme-linked immunosorbent assay. Immunocytochemistry showed the same reactivity against five cell lines (K562, Daudi, HT-180, SW480, and PC-14), whereas levels of WT1 mRNA expression determined by real-time qPCR (RT-PCR) analysis were not equivalent. Next, we examined the reactivity of WT1-R in tissue samples compared with a previously developed anti-WT1 antibody, 6F-H2. WT1-R showed greater sensitivity for detecting WT1 protein expression in samples from four different breast cancer patients than 6F-H2 antibody. The discrepancy in WT1 expression between these methods suggested that immunohistochemical detection of WT1 peptide may be advantageous for predicting the efficacy of WT1 vaccine compared to RT-PCR, and the highly sensitive WT1 antibody, WT1-R, may be useful to detect WT1 protein in tumors. (*Cancer Sci* 2010; 101: 1089–1092)

Wilms' tumor 1 (WT1) mRNA is expressed at high levels in hematological malignancies and various cancers, while normal tissue shows only low levels of its expression.[1–6] The specific overexpression of WT1 in malignant cells makes it an attractive potential target for immunotherapy, including WT1-targeting vaccine therapy.[7–11] A peptide has already been developed as a vaccine and its clinical efficacy has been evaluated.[12,13]

Precise determination of WT1 protein expression in tumors would be useful to predict the efficacy of WT1 vaccine. Although the real-time quantitative PCR (RT-PCR) method is commonly used to measure WT1 expression, it is not a direct method to evaluate expression of the target of WT1 vaccine, which is a small part of the WT1 protein. In this regard, immunohistochemical analysis using antibodies that recognize peptide sequences in WT1 protein corresponding to the peptide target of WT1 vaccine may be better correlated with efficacy of the vaccine compared to the RT-PCR method. In addition, immunohistochemical analysis is sometimes preferred to RT-PCR as most solid tumors are diagnosed by histopathological analysis of paraffin-embedded tissues. Immunohistochemical analysis has a number of benefits for estimating the efficacy of WT1 vaccine, but no antibodies for this purpose are commercially available.[14–19] Here, we developed an antibody that is specific for a peptide corresponding to the region recognized by the WT1 vaccine and examined its specificity and reactivity.

Materials and Methods

Primary antibodies. A peptide corresponding to the wild-type human WT1 (WT1 235 peptide, CMTWNQMNL) was synthesized[11] and coupled to bovine thymoglobulin as a carrier protein. This complex of peptide and protein was used as an immunogen and used to immunize three rabbits four times every 2 weeks. The sera from all rabbits showed a high anti-WT1 peptide antibody titer 1 week after the last immunization (Immuno-Biological Laboratories, Gunma, Japan). A sufficient amount of blood volume was collected from the rabbits 9 weeks after the last immunization, and the serum samples were purified using Thiol Sepharose 4B (Amersham Pharmacia Biotech, Piscataway, NJ, USA) coupled with antigen peptide. This purified solution was used as anti-WT1 antibody (WT1-R). In addition, mouse monoclonal antibodies to WT1 (clone 6F-H2; Dako Cytomation, Carpinteria, CA, USA) and to glutathione *S*-transferase (GST; clone 40B3; BioPortfolio, Dorset, UK) were also used for comparison.

Purification of recombinant WT1. GST-WT1 and GST-delWT1 were produced according to the methods described previously.[20] Briefly, full-length WT1 and part of the *WT1* gene corresponding to amino acids 180–324 were ligated into the pGEX-5X-3 vector (GE Healthcare, Buckinghamshire, UK) and transfected into *E. coli*. After collection of bacterial cells and extraction of the protein, GST-WT and GST-delWT1 protein were purified and used for western blotting analysis.

Immunoprecipitation. Aliquots of 25 μg of GST-WT1 or GST-delWT1 and GST protein were incubated with 3 μg of purified anti-WT1 polyclonal antibody at 4°C overnight, and the immune complexes were collected by incubation with protein G-Sepharose beads at 4°C for 1 h. The beads were washed with TNE buffer (10 mM Tris-HCl [pH 7.5], 0.1 M NaCl, 1 mM EDTA), and the proteins were eluted with sodium dodecyl sulfate (SDS) sample buffer.

Western blotting analysis. Denatured proteins were fractionated by SDS–polyacrylamide gel electrophoresis and subsequently blotted onto polyvinylidene difluoride membranes. The filters were blocked with PBS containing 3.3% nonfat milk, 1% bovine serum albumin, and 0.05% NaN_3 at 37°C for 2 h, and

[8]To whom correspondence should be addressed.
E-mail: ryo@mail.tains.tohoku.ac.jp

doi: 10.1111/j.1349-7006.2010.01522.x

then incubated overnight with the primary antibody. After binding of relevant peroxidase-conjugated secondary antibodies, the filters were developed with ECL (GE Healthcare).

Competitive enzyme-linked immunosorbent assay (ELISA). Ninety-six-well plates were coated with GST-WT1 protein (50 ng/well) at 4°C overnight, and then blocked with 0.1% casein in PBS at 4°C overnight. Serial dilutions of WT1 peptide were incubated with anti-WT1 antibody (WT1-R) at a concentration of 3 μg/mL at 4°C overnight. The mixtures were added to GST-WT1-coated plates and incubated at 37°C for 30 min. After incubation with peroxidase-conjugated antirabbit IgG, absorbance was determined at 492 nm with an ELISA reader.

Real-time quantitative-PCR (RT-PCR). For RT-PCR, total RNA was extracted from each cell line and reverse-transcribed using a Transcriptor First Strand cDNA Synthesis kit (Roche Diagnostics, Tokyo, Japan). Quantitative PCR was performed using a LightCycler (Roche Diagnostics) with LightCycler Fast Start DNA Master SYBR Green I (Roche Diagnostics) according to the manufacturer's protocol. The primers used for PCR were as follows. Human GAPDH forward: 5′-TGAACGGGAAGCTCACTGG-3′, reverse: 5′-TCCACCACCCTGTTGCTGTA-3′; Human WT-1 forward: 5′-CCAGGCTGCAATAAGAGATA-3′, reverse: 5′-TCTTTTGAGCTGGTCTGAA-3′. PCR for human GAPDH was performed for 40 cycles consisting of 95°C for 10 s, 60°C for 10s, and 72°C for 12 s. Human WT-1 was amplified by 40 cycles of 95°C for 10 s, 62°C for 10 s, and 72°C for 5 s.

Immunohistochemistry. For immunohistochemical staining, cells were fixed in PBS with 10% formaldehyde and then these fixed cells were embedded in agar blocks and sections were then cut using a microtome for immunostaining. Breast cancer and normal gastric mucosa specimens were obtained with informed consent (Pathology Institute Corporation, Toyama, Japan), and antigen retrieval was performed after deparaffinization of the slides by heating the sections in Tris-buffered saline, pH 9.0, in a water bath at 95°C for 40 min. Sections were allowed to cool to room temperature and endogenous peroxidase activity was blocked with 3% H_2O_2. The sections were then incubated with WT1-R or 6F-H2 as the primary antibody at a dilution of 1:500 (WT1-R) or 1:50 (6F-H2) for 30 min, followed by detection using the Dako EnVision/Polymer System (Dako, Ely, Cambridgeshire, UK). Sections were lightly counterstained with hematoxylin.

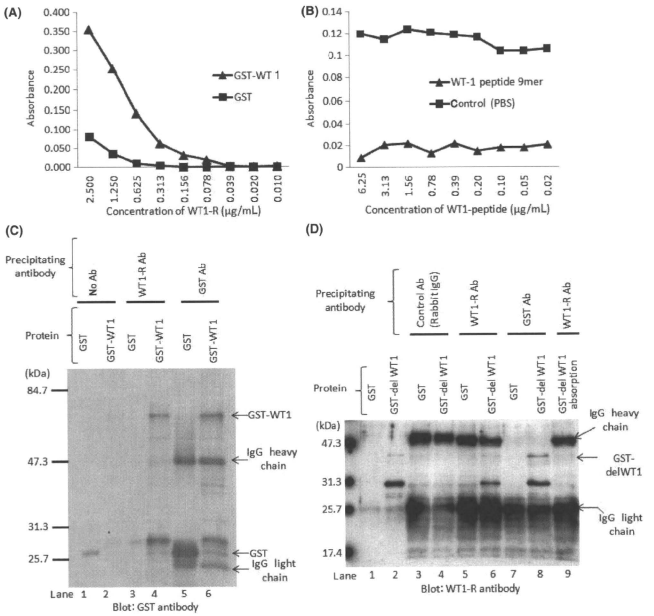

Fig. 1. Reactivity of WT1-R antibody against 9-mer peptide region of Wilms' tumor 1 (WT1) protein targeted by WT1 vaccine. (A) Dilution curves of WT1-R. Plates coated with WT1-GST or GST protein were incubated with serial dilutions of WT1-R antibody and the binding of WT1-R antibody to plates was determined. (B) Results of competitive ELISA. Serially diluted WT1 peptide was incubated with or without 3 mg/mL of WT1-R antibody, and this mixture was then added to GST-WT1-coated plates. (C,D) Western blotting analysis with GST or WT1-R antibody. Proteins were immunoprecipitated with the antibodies indicated above before electrophoresis.

doi: 10.1111/j.1349-7006.2010.01522.x

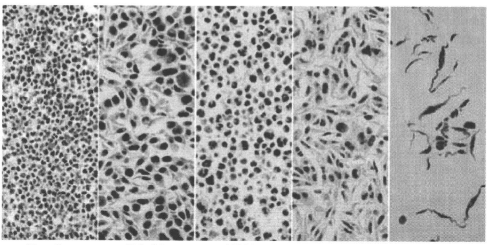

Fig. 2. Comparison between immunohistochemical staining with WT1-R and real-time quantitative PCR (RT-PCR) to detect Wilms' tumor 1 (WT1) expression in five cell lines (Daudi, PC-14, K562, HT1080, and SW480). RT-PCR results are shown beneath the photographs. Magnification, ×400.

Results

Anti-WT1 polyclonal antibody WT1-R binds specifically to GST-WT1 protein and 9-mer peptide corresponding to WT1 vaccine antigen. To assess antibody reactivity, WT1-R was serially diluted and its binding to plates coated with GST-WT1 protein and GST protein was examined. WT1-R bound strongly to GST-WT1-coated plates, whereas no binding was observed on GST-coated plates (Fig. 1A). To evaluate the specificity of WT1-R antibody, we performed competitive ELISA with WT1 peptide. As shown in Figure 1(B), antibody binding to GST-WT1 was markedly decreased by preincubation with WT1 peptide compared to control (PBS). Next, we examined antibody binding by immunoprecipitation and Western blotting analysis. As shown in Figure 1(C), GST-WT1 protein was immunoprecipitated by WT1-R and anti-GST antibodies and detected by anti-GST antibody (lanes 4 and 6). Figure 1(D) shows the results of western blotting analysis using WT1-R as the primary antibody. In this experiment, we used GST-delWT1 protein, which included the amino acid sequence targeted by WT1-R. Purified GST-delWT1 protein (lane 2) was detected by WT1-R, whereas WT1-R did not react with GST protein (lane 1). GST and GST-delWT1 protein were immunoprecipitated with control (rabbit IgG), anti-GST, or anti-GST antibody before western blotting, and WT1-R reacted only with GST-delWT1 immunoprecipitated by WT1-R (lane 6) and anti-GST antibody (lane 8). These bands disappeared when the antibodies were preincubated with 9-mer WT1-peptide before immunoprecipitation (lane 9). These results indicated that WT1-R antibody could detect WT1 protein and the binding was specific for part of WT1 protein corresponding to the 9-mer peptide used for WT1 vaccine.

Immunohistochemical analysis of WT1-R antibody. Immunohistochemical analysis of five cell lines (K562, Daudi, HT-1080, SW480, and PC-14) was performed and the results were

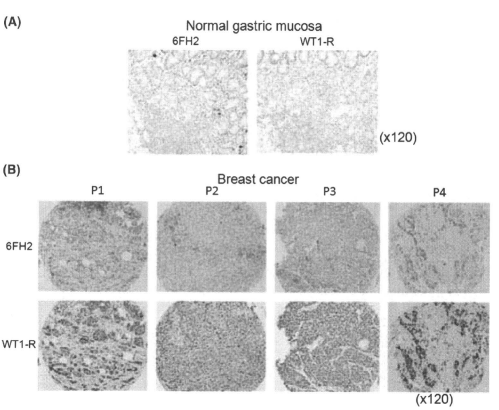

Fig. 3. Immunohistochemical analysis of normal gastric mucosa (A) and breast cancer tissue samples from four different patients (B). In (B), the upper and lower photographs show the results of immunohistochemical staining with 6F-H2 and with WT1-R, respectively. Magnification, ×120.

compared with those of RT-PCR. As shown in Figure 2, K562 (WT1 copy number/GAPDH copy number: 0.048), Daudi (0.061), and SW480 (0.042) showed about 5–6-fold higher levels of expression than HT-1080 (0.01), and the expression level in PC-14 was almost 1000-fold lower (0.000052) than in the other lines. These results indicated that the expression was not equivalent in these cell lines although they expressed WT1. On the other hand, in contrast to the difference in WT1 mRNA expression between cell lines, immunohistochemical analysis with WT1-R showed almost the same binding intensity in these cell lines (Fig. 2).

Next, we compared the reactivity of WT1-R with that of 6F-H2 antibody in normal gastric mucosa tissue and breast cancer tissue samples obtained from four different patients (Fig. 3). In normal gastric mucosa, plasma cells showed nonspecific staining with 6F-H2 antibody, but were completely negative for staining by WT1-R with no nonspecific binding (Fig. 3A). In breast cancer tissues, immunostaining with 6F-H2 showed weak positive reactivity in breast cancer samples, while staining with WT1-R was clearly positive in both the nucleus and cytoplasm of breast cancer cells and the staining intensity was significantly higher with WT1-R than in 6F-H2 (Fig. 3B). These observations indicated that WT1-R antibody is more sensitive for detection of WT1 protein in breast cancer than 6F-H2 antibody.

Discussion

RT-PCR is widely employed for determination of WT1 expression.[11,21] However, the results of RT-PCR are not always correlated with protein expression[22] and this method is not suitable for tumors that consist of cells of various types, including malignant and non-malignant cells, because the results are dependent on the proportion of malignant to normal cells. Therefore, immunohistochemical analysis of WT1 expression in solid tumors may be a better option than RT-PCR. In the present study, the results of immunohistochemical analysis of WT1 expression were not correlated with those of RT-PCR. The level of WT1 mRNA transcript expression in PC-14 was very weak, but protein expression level was almost the same as in the other cell lines. This observation suggested that WT1 mRNA expression is not equivalent to its protein expression. A discrepancy between WT1 mRNA and protein expression was reported previously in childhood leukemia.[22] These results suggested that immunohistochemical analysis is important to predict the efficacy of WT1 vaccines. The WT1-R antibody developed in the present study shows sensitivity for detection of WT1 protein and may be useful for immunohistochemical analysis.

Currently, there is no standard method for immunohistochemical analysis of WT1 because of a lack of appropriate antibodies. It has already been reported that staining results with 6F-H2 and another antibody against WT1 showed marked differences in some types of tumor.[21] The WT1-R antibody developed in the present study showed high sensitivity for detection of WT1 protein in breast cancer samples compared with 6F-H2 antibody, and may be appropriate for immunohistochemical analysis of WT1. Further studies of the sensitivity and specificity of WT1-R antibody in various types of cancer are required.

Acknowledgment

We thank Y. Tani (Pathology Institute Corporation Ltd., Toyama, Japan) for pathology specimens and performing the immunohistochemical analyses.

Disclosure Statement

The authors have no conflict of interest.

References

1 Oji Y, Miyoshi S, Maeda H *et al.* Overexpression of the Wilms' tumor gene WT1 in *de novo* lung cancers. *Int J Cancer* 2002; **100**: 297–303.
2 Ueda T, Oji Y, Naka N *et al.* Overexpression of the Wilms' tumor gene WT1 in human bone and soft-tissue sarcomas. *Cancer Sci* 2003; **94**: 271–6.
3 Oji Y, Yamamoto H, Nomura M *et al.* Overexpression of the Wilms' tumor gene WT1 in colorectal adenocarcinoma. *Cancer Sci* 2003; **94**: 712–7.
4 Oji Y, Yano M, Nakano Y *et al.* Overexpression of the Wilms' tumor gene in esophageal cancer. *Anticancer Res* 2004; **24**: 3103–8.
5 Oji Y, Suzuki T, Nakano Y *et al.* Overexpression of the Wilms' tumor gene W T1 in primary astrocytic tumors. *Cancer Sci* 2004; **95**: 822–7.
6 Oji Y, Nakamori S, Fujikawa M *et al.* Overexpression of the Wilms' tumor gene WT1 in pancreatic ductal adenocarcinoma. *Cancer Sci* 2004; **95**: 583–7.
7 Oka Y, Udaka K, Tsuboi A *et al.* Cancer immunotherapy targeting Wilms' tumor gene WT1 product. *J Immunol* 2000; **164**: 1873–80.
8 Oka Y, Tsuboi A, Elisseeva OA, Udaka K, Sugiyama H. WT1 as a novel target antigen for cancer immunotherapy. *Curr Cancer Drug Targets* 2002; **2**: 45–54.
9 Nakajima H, Kawasaki K, Oka Y *et al.* WT1 peptide vaccination combined with BCG-CWS is more efficient for tumor eradication than WT1 peptide vaccination alone. *Cancer Immunol Immunother* 2004; **53**: 617–24.
10 Oka Y, Tsuboi A, Taguchi T *et al.* Induction of WT1 (Wilms' tumor gene)-specific cytotoxic T lymphocytes by WT1 peptide vaccine and the resultant cancer regression. *Proc Natl Acad Sci U S A* 2004; **101**: 13885–90.
11 Oka Y, Tsuboi A, Kawakami M *et al.* Development of WT1 peptide cancer vaccine against hematopoietic malignancies and solid cancers. *Curr Med Chem* 2006; **13**: 2345–52.
12 Morita S, Oka Y, Tsuboi A *et al.* A phase I/II trial of a WT1 (Wilms' tumor gene) peptide vaccine in patients with solid malignancy: safety assessment based on the phase I data. *Jpn J Clin Oncol* 2006; **36**: 231–6.
13 Izumoto S, Tsuboi A, Oka Y *et al.* Phase II clinical trial of Wilms tumor 1 peptide vaccination for patients with recurrent glioblastoma multiforme. *J Neurosurg* 2008; **108**: 963–71.
14 Foster MR, Johnson JE, Olson SJ, Allred DC. Immunohistochemical analysis of nuclear versus cytoplasmic staining of WT1 in malignant mesotheliomas and primary pulmonary adenocarcinomas. *Arch Pathol Lab Med* 2001; **125**: 1316–20.
15 Chen BF, Tzen CY, Liang DC, Liu HC, Huang YW, Fan CC. Immunohistochemical expression of Wilms' tumor 1 protein in nephroblastoma. *J Chin Med Assoc* 2004; **67**: 506–10.
16 Waldstrøm M, Grove A. Immunohistochemical expression of Wilms tumor gene protein in different histologic subtypes of ovarian carcinomas. *Arch Pathol Lab Med* 2005; **129**: 85–8.
17 Wilsher M, Cheerala B. WT1 as a complementary marker of malignant melanoma: an immunohistochemical study of whole sections. *Histopathology* 2007; **51**: 605–10.
18 Kushitani K, Takeshima Y, Amatya VJ, Furonaka O, Sakatani A, Inai K. Immunohistochemical marker panels for distinguishing between epithelioid mesothelioma and lung adenocarcinoma. *Pathol Int* 2007; **57**: 190–9.
19 Ellison DA, Parham DM, Bridge J, Beckwith JB. Immunohistochemistry of primary malignant neuroepithelial tumors of the kidney: a potential source of confusion? A study of 30 cases from the National Wilms Tumor Study Pathology Center. *Hum Pathol* 2007; **38**: 205–11.
20 Oji Y, Kitamura Y, Kamino E *et al.* WT1 IgG antibody for early detection of nonsmall cell lung cancer and as its prognostic factor. *Int J Cancer* 2009; **125**: 381–7.
21 Nakatsuka S, Oji Y, Horiuchi T *et al.* Immunohistochemical detection of WT1 protein in a variety of cancer cells. *Mod Pathol* 2006; **19**: 804–14.
22 Kerst G, Bergold N, Gieseke F *et al.* WT1 protein expression in childhood acute leukemia. *Am J Hematol* 2008; **83**: 382–6.

doi: 10.1111/j.1349-7006.2010.01522.x

Author Affiliations: Ophthalmic Plastic and Reconstructive Surgery Division (Drs Fay and Nguyen) and Cogan Ophthalmic Pathology Laboratory (Dr Jakobiec), Harvard Medical School, Massachusetts Eye and Ear Infirmary, Boston; Center for Vascular Malformation in Children, St Joseph Hospital, Berlin, Germany (Dr Meyer-Junghaenel); and Vascular Birthmark Institute of New York, St Luke's/Roosevelt Hospital Center, New York (Dr Waner). Dr Nguyen is now with the Department of Ophthalmology, Robert C. Byrd Health Science Center, West Virginia University School of Medicine, Morgantown.
Correspondence: Dr Fay, Massachusetts Eye and Ear Infirmary, 243 Charles St, Boston, MA 02114 (aaron_fay@meei.harvard.edu).
Financial Disclosure: None reported.

1. Goldberg NS, Rosanova MA. Periorbital hemangiomas. *Dermatol Clin*. 1992; 10(4):653-661.
2. Haik BG, Karcioglu ZA, Gordon RA, Pechous BP. Capillary hemangioma (infantile periocular hemangioma). *Surv Ophthalmol*. 1994;38(5):399-426.
3. Léauté-Labrèze C, Dumas de la Roque E, Hubiche T, Boralevi F, Thambo JB, Taieb A. Propranolol for severe hemangiomas of infancy. *N Engl J Med*. 2008; 358(24):2649-2651.

Ocular Involvement by Epstein-Barr Virus–Positive Diffuse Large B-Cell Lymphoma of the Elderly: A New Disease Entity in the World Health Organization Classification

The new World Health Organization classification of lymphoma places great emphasis on the definition of real biological disease entities in the category of diffuse large B-cell lymphoma (DLBCL). Epstein-Barr virus (EBV)–positive DLBCL of the elderly is a new subtype of DLBCL according to the 2008 World Health Organization classification. This is an extremely rare tumor, and no case of ocular EBV-positive DLBCL of the elderly has been reported to our knowledge. Here we describe the first case of EBV-positive DLBCL of the elderly with involvement of the eyelid and orbit.

Report of a Case. An 83-year-old woman was referred with an eyelid tumor of her left eye. Serologically, human immunodeficiency virus antigen and anti–human T-cell lymphoma virus 1 antigen were both negative. The left upper and lower eyelids were affected by a hyperemic tumor with a rough surface and a small scab, which caused ectropion (**Figure 1**A and B). Physical examination revealed that her left submandibular, parotid, and cervical lymph nodes were enlarged. Staging examination showed that she had stage III B-cell malignant lymphoma according to the Ann Arbor classification. Orbital magnetic resonance imaging revealed a cystic mass in the left periorbital region, invading the orbit and the anterior ethmoid sinus (Figure 1F and G). Incisional biopsy of the left eyelid lesion was performed, revealing a tumor composed of pleomorphic large cells and marked by the presence of mononuclear Hodgkin-like cells and multinucleated Reed-Sternberg–like cells (**Figure 2**A and B). Immunohistochemistry revealed that the tumor cells expressed CD20 (Figure 2C), Pax-5 (Figure 2D), CD30 (Figure 2E), and multiple myeloma oncogene 1 protein (not shown). The tumor cells were also positive for latent membrane protein 1 (Figure 2F) but negative for EBV nuclear antigen 2 (not shown), indicating that the EBV infection pattern in this case was type 2 latency. Staining results for CD5, CD10, and the follicular B-cell lymphoma marker bcl-6 were negative (not shown). Based on these findings, a diagnosis of EBV-positive DLBCL of the elderly was made according to the new World Health Organization lymphoma classification. Cervical lymph node involvement was also confirmed by biopsy. Immediately after the biopsy, the patient received standard chemotherapy with rituximab, cyclophosphamide, doxorubicin hydrochloride, vincristine sulfate, and prednisone, followed by rituximab and

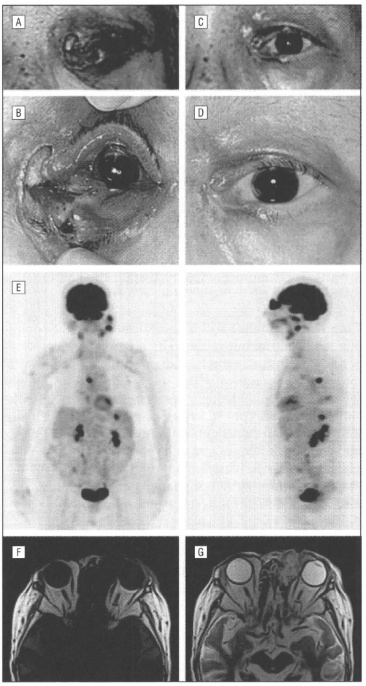

Figure 1. Images from a patient with Epstein-Barr virus–positive diffuse large B-cell lymphoma of the elderly. A and B, Before starting chemotherapy. C and D, After completion of chemotherapy. E, Positron emission tomography confirms marked left orbital uptake. There is also uptake in the spleen, mediastinum, and involved lymph nodes. F and G, Orbital magnetic resonance imaging shows a cystic mass in the left periorbital region that invades the orbit and anterior ethmoid sinus and is accompanied by eyelid ulceration. The mass shows heterogeneous low signal intensity on a T1-weighted axial image (F) and high signal intensity on a T2-weighted axial image (G).

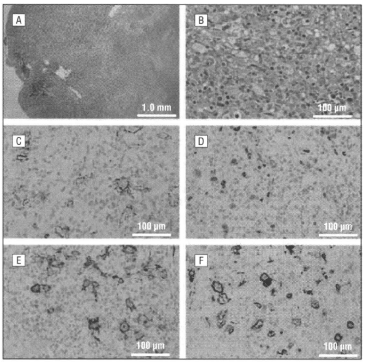

Figure 2. Histological examination findings from the eyelid of a patient with Epstein-Barr virus–positive diffuse large B-cell lymphoma of the elderly. A, A diffuse lymphoid infiltrate with necrosis can be seen at low power (hematoxylin-eosin). B, At higher power, the infiltrate comprises large and pleomorphic tumor cells, including Hodgkinlike cells and Reed-Sternberg–like giant cells, with a background of smaller reactive inflammatory cells (hematoxylin-eosin). The tumor cells express B-cell markers CD20 (C) and Pax-5 (D), while CD30 (E) and latent membrane protein 1 (F) are also positive.

etoposide. She achieved near complete remission after 4 months of chemotherapy. During the subsequent 4 months, there has been no evidence of local recurrence.

Comment. Epstein-Barr virus–associated B-cell lymphomas have been mainly reported in immunosuppressed patients such as those with human immunodeficiency virus infection, organ transplantation, or methotrexate therapy for rheumatoid arthritis.[1] Epstein-Barr virus–positive DLBCL of the elderly is defined as a lymphoproliferative disorder arising in patients without predisposing immunodeficiency, including human immunodeficiency virus and human T-cell lymphoma virus 1 infection, a history of chemotherapy or radiotherapy, and autoimmune disease, and is thought to result from immunological deterioration associated with aging.[2,3] According to the World Health Organization classification, EBV-positive DLBCL of the elderly is a rare DLBCL that accounts for 8% to 10% of DLBCL among patients without predisposing immunodeficiency in Asian countries.[4] Interestingly, EBV-positive DLBCL of the elderly frequently involves extranodal sites.[3,5] Most patients with extranodal disease also have nodal disease. In fact, 70% of patients have extranodal disease affecting sites such as the skin, lung, tonsils, or stomach, while 30% of patients have lymph node involvement alone.[4] However, no case of ocular involvement, which is an extranodal site, has been reported. To our knowledge, our case is the first report of EBV-positive DLBCL of the elderly involving the eyelid and orbit.

Epstein-Barr virus–positive DLBCL of the elderly with ocular involvement is totally distinct, both clinically and pathologically, from extranodal marginal zone B-cell lymphoma of mucosa-associated lymphoid tissue, an indolent tumor that is the most common form of lymphoma in the orbital region. Although relatively uncommon, EBV-positive DLBCL of the elderly should be considered in the differential diagnosis of ocular lymphoma since it needs to be treated appropriately as a highly aggressive lymphoma.

Hideki Tsuji, MD
Megumi Tamura, MD
Masahiro Yokoyama, MD
Kengo Takeuchi, MD
Tatsuya Mimura, MD

Author Affiliations: Departments of Ophthalmology (Drs Tsuji and Tamura) and Medical Oncology and Hematology (Dr Yokoyama) and Division of Pathology (Dr Takeuchi), The Cancer Institute Hospital of JFCR, and Department of Ophthalmology, University of Tokyo Graduate School of Medicine (Drs Tsuji and Mimura), Tokyo, Japan.
Correspondence: Dr Tsuji, Department of Ophthalmology, The Cancer Institute Hospital of JFCR, 3-10-6 Ariake, Kouto-ku, Tokyo 135-8550, Japan (tsuji-tky@umin.ac.jp).
Author Contributions: Dr Tsuji had full access to all of the data in the study and takes responsibility for the integrity of the data and the accuracy of the data analysis.
Financial Disclosure: None reported.
Funding/Support: This work was supported by a grant-in-aid for scientific research from the Ministry of Education, Culture, Sports, Science, and Technology of Japan.

1. Purtilo DT, Tatsumi E, Monolov G, Monolova Y, Harada S, Lipscomb H. Epstein-Barr virus as an etiological agent in the pathogenesis of lymphoproliferative and aproliferative diseases in immune deficient patients. In: Richter GW, Epstein MA, eds. *International Review of Experimental Pathology*. Orland, FL: Academic Press; 1985:113.
2. Oyama T, Ichimura K, Suzuki R, et al. Senile EBV+ B-cell lymphoproliferative disorders: a clinicopathologic study of 22 patients. *Am J Surg Pathol*. 2003; 27(1):16-26.
3. Oyama T, Yamamoto K, Asano N, et al. Age-related EBV-associated B-cell lymphoproliferative disorders constitute a distinct clinicopathologic group: a study of 96 patients. *Clin Cancer Res*. 2007;13(17):5124-5132.
4. Nakamura S, Jaffe ES, Swerdlow SH. EBV positive diffuse large B-cell lymphoma of the elderly. In: Swerdlow SH, Campo E, Harris NL, eds, et al. *WHO Classification of Tumours of Haematopoietic and Lymphoid Tissues*. 4th ed. Lyon, France: IARC Press; 2008:243-244.
5. Shimoyama Y, Oyama T, Asano N, et al. Senile Epstein-Barr virus-associated B-cell lymphoproliferative disorders: a mini review. *J Clin Exp Hematop*. 2006; 46(1):1-4.

Severe Retinal Vascular Infarction After Photodynamic Therapy With Verteporfin Using the Standard Protocol

Photodynamic therapy (PDT) with verteporfin has been widely used for the treatment of choroidal neovascularization associated with age-related macular degeneration, with both the efficacy and safety of PDT considered to be at tolerable levels. Herein, we describe a patient who experienced severe retinal vascular infarction exactly corresponding to the irradiated spot following PDT using the standard protocol.

Report of a Case. A 60-year-old man was referred because of decreased vision in the right eye. He had a history of diabetes mellitus, systemic hypertension, arteriosclerosis obliterans, and renal failure requiring dialysis. The right

The American Journal of Pathology, Vol. 176, No. 3, March 2010

DOI: 10.2353/ajpath.2010.091057

Correspondence

EML4-ALK Fusion in Lung

To the Editor-in-Chief:

The recent article by Martelli et al[1] reports (i) the detection of *EML4-ALK* fusion cDNA[2] not only in non-small cell lung cancer (NSCLC) specimens but in non-tumor lung tissues, (ii) a very low proportion of FISH-positive cells for *ALK* rearrangements among *EML4-ALK*–positive specimens, and (iii) the failure to detect EML4-ALK protein by immunohistochemistry (IHC) and Western blotting. Based on these lines of observation, the authors questioned the clinical relevance of *EML4-ALK* in the carcinogenesis of NSCLC.

Although detection of fusion kinases in normal tissues is a potentially interesting observation, caution is warranted in the interpretation of their results.[1,3] They replicated thrice the reverse transcription-polymerase chain reaction (RT-PCR) for *EML4-ALK* and noted that "In half of the (positive) cases, one replicate experiment did not confirm the fusion transcript was present." They then suggested that the fusion gene was "expressed at very low level." It is, however, also quite possible that such unstable PCR results may simply represent contaminated experiments. If this is the case, a discussion on FISH and protein analyses would become irrelevant. In their report, the presence of the *EML4-ALK* fusion gene was only evidenced by unstable RT-PCR results and a small proportion of FISH-positive cells among specimens.

In this regard, it was surprising that the authors had not tried genomic PCR to exclude the possibility of PCR contamination.[1,3] In most of their fusion-positive cases, they found the *EML4-ALK* variant 1 cDNA, in which exon 13 of *EML4* cDNA is connected to exon 20 of *ALK* cDNA. Because the length of intron 14 of *EML4* gene and intron 19 of *ALK* gene is 5724 bp and 1932 bp, respectively, the maximum size of the genomic PCR to detect the gene fusion should be ≈7.7 kbp, which is within the scope of current long-range PCR systems. Indeed, we have been able to detect genomic PCR products among >50% of the fusion cDNA-positive cases. Interestingly, the break/fusion points in the genome vary substantially among NSCLC specimens,[2,4,5] and we have not obtained, to date, any pairs of NSCLC specimens carrying identical break/fusion points in their genome (even among those positive for the same *EML4-ALK* variants).

We speculate, therefore, that (i) if none of the fusion cDNA-positive cases reported by Martelli et al[1,3] produce specific genomic PCR products, then the fusion cDNA products likely arose from cDNA-contamination, (ii) if the fusion cDNA–positive cases yield identical genomic PCR products, then the fusion cDNAs likely arose from specimen-contamination, and (iii) if the fusion cDNA-positive cases display distinct genomic fusion points, then each specimen was truly positive for the *EML4-ALK* fusion gene. Without such careful examination, we have to conclude that their claims in the article have not as yet been clearly demonstrated.

As described previously,[6] immunohistochemical detection of the EML4-ALK protein is highly difficult, probably owing to the weak activity of the *EML4* promoter that drives the expression of *EML4-ALK* messages. We have thus examined the suitability of commercially available antibodies to ALK for IHC and successfully developed the intercalated antibody–enhanced polymer (iAEP) method, which enables reliable detection of EML4-ALK among formalin-fixed and paraffin-embedded specimens.[6] The same specimen positive for *EML4-ALK* RT-PCR can be, for instance, readily stained to be positive with iAEP, but negative with conventional IHC methods (see Supplemental Figure S1 in Ref. 6). We thus agree with Martelli et al that screening of NSCLC specimens with conventional IHC methods will not detect EML4-ALK protein, but strongly argue that such failure does not simply indicate the absence of EML4-ALK. For such screening, we recommend iAEP or other sensitive techniques.[7]

It should be further noted that, in both our[6] and other researchers' IHC analyses,[7] almost all tumor cells in a given *EML4-ALK*–positive specimen were positively immunostained with anti-ALK antibodies, suggesting a homogenous presence of *EML4-ALK* within a tumor. Such observation is, however, in contrast to the FISH data by Martelli et al, which show that the *ALK* rearrangement was only positive in ≈2% of tumor cells in a given *EML4-ALK*–positive specimen. On the contrary, FISH analyses of our *EML4-ALK*–positive samples clearly demonstrate that most of the tumor cells harbor rearranged *ALK* alleles, implying that the generation of the *EML4-ALK* fusion gene is an early event in NSCLC carcinogenesis. The homogenous presence of EML4-ALK in our fusion-positive tumors, as demonstrated by both FISH and IHC, further raises a concern about the "EML4-ALK–positive tumors" as defined by Martelli et al.

Specific inhibitors to ALK enzymatic activity are already in clinical trial, as reported at the 2009 annual meeting of America Society of Clinical Oncology and the European Cancer Organization and Congress of the European Society for Medical Oncology.[8] Such reports reveal only

modest and transient side effects (nausea, vomiting, and diarrhea) with their ALK inhibitor, but without severe damage in hematopoiesis or renal function. On the other hand, the marked therapeutic efficacy of their compound against EML4-ALK–positive NSCLC makes it one of the rare, highly successful molecular targeted therapies against human cancer, in line with imatinib mesylate and gefitinib/erlotinib. These data further reinforce the essential role of EML4-ALK in the carcinogenesis of NSCLC, and question the validity of the conclusions led by Martelli et al.[1,3]

Hiroyuki Mano

The University of Tokyo
Tokyo, Japan

Kengo Takeuchi

The Cancer Institute
Tokyo, Japan

References

1. Martelli MP, Sozzi G, Hernandez L, Pettirossi V, Navarro A, Conte D, Gasparini P, Perrone F, Modena P, Pastorino U, Carbone A, Fabbri A, Sidoni A, Nakamura S, Gambacorta M, Fernandez PL, Ramirez J, Chan JK, Grigioni WF, Campo E, Pileri SA, Falini B: EML4-ALK rearrangement in non-small cell lung cancer and non-tumor lung tissues. Am J Pathol 2009, 174:661–670
2. Soda M, Choi YL, Enomoto M, Takada S, Yamashita Y, Ishikawa S, Fujiwara S, Watanabe H, Kurashina K, Hatanaka H, Bando M, Ohno S, Ishikawa Y, Aburatani H, Niki T, Sohara Y, Sugiyama Y, Mano H: Identification of the transforming *EML4-ALK* fusion gene in non-small-cell lung cancer. Nature 2007, 448:561–566
3. Sozzi G, Martelli MP, Conte D, Modena P, Pettirossi V, Pileri SA, Falini B: The EML4-ALK transcript but not the fusion protein can be expressed in reactive and neoplastic lymphoid tissues. Haematologica 2009, 94:1307–1311
4. Choi YL, Takeuchi K, Soda M, Inamura K, Togashi Y, Hatano S, Enomoto M, Hamada T, Haruta H, Watanabe H, Kurashina K, Hatanaka H, Ueno T, Takada S, Yamashita Y, Sugiyama Y, Ishikawa Y, Mano H: Identification of novel isoforms of the *EML4-ALK* transforming gene in non-small cell lung cancer. Cancer Res 2008, 68:4971–4976
5. Takeuchi K, Choi YL, Soda M, Inamura K, Togashi Y, Hatano S, Enomoto M, Takada S, Yamashita Y, Satoh Y, Okumura S, Nakagawa K, Ishikawa Y, Mano H: Multiplex reverse transcription-PCR screening for *EML4-ALK* fusion transcripts. Clin Cancer Res 2008, 14:6618–6624
6. Takeuchi K, Choi YL, Togashi Y, Soda M, Hatano S, Inamura K, Takada S, Ueno T, Yamashita Y, Satoh Y, Okumura S, Nakagawa K, Ishikawa Y, Mano H: KIF5B-ALK, a novel fusion oncokinase identified by an immunohistochemistry-based diagnostic system for ALK-positive lung cancer. Clin Cancer Res 2009, 15:3143–3149
7. Rodig SJ, Mino-Kenudson M, Dacic S, Yeap BY, Shaw A, Barletta JA, Stubbs H, Law K, Lindeman N, Mark E, Janne PA, Lynch T, Johnson BE, Iafrate AJ, Chirieac LR: Unique clinicopathologic features characterize ALK-rearranged lung adenocarcinoma in the western population. Clin Cancer Res 2009, 15:5216–5223
8. Kwak EL, Camidge DR, Clark J, Shapiro GI, Maki RG, Ratain MJ, Solomon B, Bang Y, Ou S, Salgia R: Clinical activity observed in a phase I dose escalation trial of an oral c-met and ALK inhibitor, PF-02341066. J Clin Oncol 2009, 27:15s, (suppl. abstr 3509)

Authors' reply:

In their letter, Mano and Takeuchi claim that our unstable PCR results in normal and cancerous lung tissues could be attributable to contamination. However, as clearly illustrated in our article,[1] serial dilution experiments in the H2228 cell line demonstrate the specificity and sensitivity of our RT-PCR assay. Furthermore, the identification in our EML4-ALK fusion positive tissues of alternative isoforms of variant 3, rather than the described two isoforms coexpressed in the H2228 cell line, is indicative of exclusive events in tumors, making contamination unlikely. Lastly, our experiments were confirmed independently in two laboratories (Milan and Barcelona) and always contained appropriate negative PCR controls.

We disagree with Mano et al's claim that the results of genomic PCR could be used to prove a possible RT-PCR contamination in our samples, which can only be excluded by the use of appropriate controls and procedures, as outlined above. However, we used genomic PCR to amplify the sequence flanking the *EML4-ALK* variant 1 breakpoint in four positive NSCLC samples. Even though a strong amplification product had been obtained from the same DNA templates using primer sets amplifying a control genomic locus of similar size to that of the cases so far reported in literature, no amplification of the *EML4-ALK* variant 1 fusion product was identified, suggesting only a minority of cells carried the *EML4-ALK* gene. These findings concur with Maes et al[2] who reported that, in lymphoid tissues, high level detection of *NPM-ALK* and *ATIC-ALK* fusion transcripts coincided with *ALK* gene rearrangements (as detected by cytogenetics and FISH), whereas low-level detection was not supported by genomic evidence of rearrangements.

In our article,[1] we clearly stated that, unlike observations in ALK+ lymphomas, tumor cells from NSCLC specimens expressed such a low amount of the EML4-ALK fusion protein that immunoprecipitation and immunohistochemistry performed with the commercially available antibodies are unable to detect it. This is in keeping with the observation that the EML4-ALK fusion protein is detectable only using highly sensitive methods, such as mass spectrometry[3] or the intercalated antibody-enhanced polymer (iAEP) method[4] which, unfortunately, are not available in all pathology laboratories and are difficult to standardize. Therefore, the question of how best to detect the EML4-ALK fusion protein remains unanswered.

Issues concerning the frequency, heterogeneity, and tissue specificity of the *EML4-ALK* rearrangement must also be addressed carefully.

Frequency

We recently extended our FISH analysis to 173 surgically resected lung cancer specimens (mainly adenocarcinoma) from an unselected group of Caucasian patients. The incidence of truly positive cases (>50% FISH positive, fusion transcript, and protein positive) was only 0.6% (1/173 cases), which reinforces the results in our artile and is in keeping with Rodig et al's[5] recent report of 1/227 (0.45%) ALK rearranged case in a series of surgically treated Western adenocarcinoma.

Heterogeneity

The heterogeneity of the *EML4-ALK* rearrangement we detected by FISH was confirmed by others in primary tumors and cell lines[6,7] and is supported by functional studies showing that the magnitude of growth inhibition by siRNA-

mediated silencing did not correlate with the number of cells harboring the rearrangement and the lack of growth inhibition in 50% of *EML4-ALK*–positive cell lines. These observations suggest that additional signaling mechanisms independent of ALK may regulate growth and cell proliferation.

Specificity

Claims from Mano's group that the *EML4-ALK* product is specific for NSCLC is contradicted by our findings in normal tissues[1,8] and by a recent study from Lin E. et al,[6] who found *EML4-ALK* fusions in breast (2.4%) and colorectal (2.4%) cancer, in addition to NSCLC.

Finally, we wonder whether it is really appropriate to compare treatments such as ALK inhibitors in NSCLC with imatinib mesylate and gefinitinib/erlotinib in other human neoplasms. In fact: i) the role of EML4-ALK in NSCLC is not as well established as that of BCR/ABL in chronic myeloid leukemia (CML); ii) NSCLC responses to ALK inhibitors[9] are not as remarkable as the CML response to imatinib mesylate; and iii) patients with NSCLC were treated with a multikinase, c-MET and ALK, inhibitor.[9] Considering that about 20% of NSCLC have MET amplification and overexpression and that MET rearrangements are homogeneous in lung cancer,[10] it may be possible that responses to the multikinase inhibitor may be related to other coexisting oncogenic events, independently of ALK.

In conclusion, although we fully acknowledge the importance of Soda et al's discovery,[11] we believe that additional studies are required to elucidate the concurrent genetic events and cellular settings necessary for *EML4-ALK* to exert an oncogenic function and to better define the role of *EML4-ALK* in diagnosis and targeted therapy of NSCLC.

Brunangelo Falini
Maria Paola Martelli

University of Perugia
Perugia, Italy

Stefano A. Pileri

University of Bologna
Bologna, Italy

Gabriella Sozzi
Patrizia Gasparini

Istituto Nazionale dei Tumori
Milan, Italy

References

1. Martelli MP, Sozzi G, Hernandez L, Pettirossi V, Navarro A, Conte D, Gasparini P, Perrone F, Modena P, Pastorino U, Carbone A, Fabbri A, Sidoni A, Nakamura S, Gambacorta M, Fernandez PL, Ramirez J, Chan JK, Grigioni WF, Campo E, Pileri SA, Falini B: EML4-ALK rearrangement in non-small cell lung cancer and non-tumor lung tissues. Am J Pathol 2009, 174:661–670
2. Maes B, Vanhentenrijk V, Wlodarska I, Cools J, Peeters B, Marynen P, de Wolf-Peeters C: The NPM-ALK and the ATIC-ALK fusion genes can be detected in non-neoplastic cells. Am J Pathol 2001, 158: 2185–2193
3. Rikova K, Guo A, Zeng Q, Possemato A, Yu J, Haack H, Nardone J, Lee K, Reeves C, Li Y, Hu Y, Tan Z, Stokes M, Sullivan L, Mitchell J, Wetzel R, Macneill J, Ren JM, Yuan J, Bakalarski CE, Villen J, Kornhauser JM, Smith B, Li D, Zhou X, Gygi SP, Gu TL, Polakiewicz RD, Rush J, Comb MJ: Global survey of phosphotyrosine signaling identifies oncogenic kinases in lung cancer. Cell 2007, 131:1190–1203
4. Takeuchi K, Choi YL, Togashi Y, Soda M, Hatano S, Inamura K, Takada S, Ueno T, Yamashita Y, Satoh Y, Okumura S, Nakagawa K, Ishikawa Y, Mano H: KIF5B-ALK, a novel fusion oncokinase identified by an immunohistochemistry-based diagnostic system for ALK-positive lung cancer. Clin Cancer Res 2009, 15:3143–3149
5. Rodig SJ, Mino-Kenudson M, Dacic S, Yeap BY, Shaw A, Barletta JA, Stubbs H, Law K, Lindeman N, Mark E, Janne PA, Lynch T, Johnson BE, Iafrate AJ, Chirieac LR: Unique clinicopathologic features characterize ALK-rearranged lung adenocarcinoma in the western population. Clin Cancer Res 2009, 15:5216–5223
6. Lin E, Li L, Guan Y, Soriano R, Rivers CS, Mohan S, Pandita A, Tang J, Modrusan Z: Exon array profiling detects EML4-ALK fusion in breast, colorectal, and non-small cell lung cancers. Mol Cancer Res 2009, 7:1466–1476
7. Perner S, Wagner PL, Demichelis F, Mehra R, Lafargue CJ, Moss BJ, Arbogast S, Soltermann A, Weder W, Giordano TJ, Beer DG, Rickman DS, Chinnaiyan AM, Moch H, Rubin MA: EML4-ALK fusion lung cancer: a rare acquired event. Neoplasia 2008, 10:298–302
8. Sozzi G, Martelli MP, Conte D, Modena P, Pettirossi V, Pileri SA, Falini B: The EML4-ALK transcript but not the fusion protein can be expressed in reactive and neoplastic lymphoid tissues. Haematologica 2009, 94:1307–1311
9. Kwak E, Camidge D, Clark J, Shapiro G, Maki R, Ratain M, Solomon B, Bang Y, Ou S, Salgia R: Clinical acitvity observed in a phase I dose escalation trial of an oral c-met and ALK inhibitor, PF-02341066. J Clin Oncol 2009, 27:15s (Suppl, Abstr 3509)
10. Beau-Faller M, Ruppert AM, Voegeli AC, Neuville A, Meyer N, Guerin E, Legrain M, Mennecier B, Wihlm JM, Massard G, Quoix E, Oudet P, Gaub MP: MET gene copy number in non-small cell lung cancer: molecular analysis in a targeted tyrosine kinase inhibitor naive cohort. J Thorac Oncol 2008, 3:331–339
11. Soda M, Choi YL, Enomoto M, Takada S, Yamashita Y, Ishikawa S, Fujiwara S, Watanabe H, Kurashina K, Hatanaka H, Bando M, Ohno S, Ishikawa Y, Aburatani H, Niki T, Sohara Y, Sugiyama Y, Mano H: Identification of the transforming EML4-ALK fusion gene in non-small-cell lung cancer. Nature 2007, 448:561–566

Manuscript Information	
Journal Acronym	GLAL
Volume and issue	
Author name	
Manuscript No. (if applicable)	_A_444456

Leukemia & Lymphoma

Typeset by
KnowledgeWorks Global Ltd.
for
informa
healthcare

QUERIES: to be answered by AUTHOR

AUTHOR: The following queries have arisen during the editing of your manuscript. Please answer the queries by making the necessary corrections on the CATS online corrections form. Once you have added all your corrections, please press the **SUBMIT** button.

QUERY NO.	QUERY DETAILS
1	A declaration of interest statement reporting no conflict of interest has been inserted. Please confirm the statement is accurate.

Manuscript Information	
Journal Acronym	GLAL
Manuscript (CATS) ID	_A_444456

Leukemia & Lymphoma

Typeset by
KnowledgeWorks Global Ltd.
for
informa
healthcare

COLOR IN PRINT REQUEST FORM

There are no color charges for ***Commentaries, Invited Reviews or Teaching Cases.*** Color will automatically be present in print and online, so authors of these manuscript types can disregard this form.

All other authors:

Please complete and return with your proof corrections if your paper contains potential color images in print.

Color costs for this journal are as follows:

Please note: If requested/possible at proof stage we can group images from various pages onto one page to potentially reduce color costs. Please give guidance in your proof corrections if this is the case. Color costs are by PAGE not per image, and size has no relevance.

- $1000 (USD) = 1st page of color
- $500 (USD) = following 3 pages of color

A custom quote will have to be provided for any manuscript with more than 4 pages of color. This will be sent to you on return of this form via e-mail for consideration. If color figures are essential to the scientific content of the manuscript, and it is not possible for the authors to cover the required charges, please contact the publishers to discuss the circumstances.

WOULD YOU LIKE TO PAY FOR COLOR IMAGES IN YOUR MANUSCRIPT?

NO THANK YOU ☐ YES, PLEASE SEE DETAILS BELOW IN SECTION 2 ☐

If you have declined color printing please ensure that all figures/images and legends are suitably amended to be read, and understood, in black and white. It is the author's responsibility to provide satisfactory alternatives at proof stage.

Please access the instructions for authors for further guidance on figure quality at: www.informaworld.com/glal

SECTION 2 - COLOR IMAGES PAYMENT DETAILS

PLEASE DETAIL THE FIGURE/IMAGE NUMBERS FOR COLOR PRINTING:

NUMBER OF COLOR PAGES: --------- / ---------- @ $1000(1st page) --------- @ $500

TOTAL COLOR COSTS: ----------

INVOICE SHOULD BE SENT TO: ----------

ADDRESS: ----------

Signed ---------- Date ----------

Please note: All invoices will be sent when the issue containing your paper is sent to the printers.
All figures/images will appear in color for free online to subscribers and purchasers.

Leukemia & Lymphoma, Month 2009; 00(0): 1–5

informa
healthcare

ORIGINAL ARTICLE

SUVmax in FDG-PET at the biopsy site correlates with the proliferation potential of tumor cells in non-Hodgkin lymphoma

REINA WATANABE[1], NAOTO TOMITA[1], KENGO TAKEUCHI[2], SEIJI SAKATA[2], UKIHIDE TATEISHI[3], MASATSUGU TANAKA[1], HIROYUKI FUJITA[1], YOSHIAKI INAYAMA[4], & YOSHIAKI ISHIGATSUBO[1]

[1]*Department of Internal Medicine and Clinical Immunology, Yokohama City University Graduate School of Medicine, Yokohama, Japan,* [2]*Department of Pathology, The Cancer Institute of Japanese Foundation for Cancer Research, Tokyo, Japan, Departments of Radiology*[3] *and* [4]*Pathology, Yokohama City University Graduate School of Medicine, Yokohama, Japan*

(Received 29 July 2009; revised 18 October 2009; accepted 26 October 2009)

Abstract

The maximum standard uptake value (SUVmax) of the whole body on 18F-fluorodeoxyglucose positron emission tomography (FDG-PET) reflects the tumor aggressiveness in non-Hodgkin lymphoma (NHL). To clarify the correlation between SUVmax at the biopsy site and the proliferation potential of tumor cells, we studied 36 patients with untreated NHL and five with untreated Hodgkin lymphoma (HL) by measuring the Ki-67 proliferation index (MIB-1 labeling index) in biopsy specimens. The measured MIB-1 labeling index was categorized into seven levels: nearly 0%, 5–20%, 21–40%, 41–60%, 61–80%, 81–95%, and nearly 100%. Twenty-four lymph nodes (LNs) and 17 extranodal (EN) sites were biopsied. The reviewed diagnosis was eight indolent lymphomas, two mantle-cell lymphomas, 26 aggressive lymphomas, and five HLs. A positive correlation was observed between the SUVmax at the biopsy site and the MIB-1 labeling index in the 36 patients with NHL ($r = 0.69$, $P < 0.001$). The correlations were also observed in LN group ($r = 0.60$, $P = 0.006$) and EN group ($r = 0.87$, $P < 0.001$), respectively. In the five patients with HL, the MIB-1 labeling index was uniformly categorized in nearly 100%. The SUVmax correlates with the proliferation potential in the case of NHL.

Keywords: *MIB-1 labeling index, non-Hodgkin lymphoma, positron emission tomography, proliferation potential, SUVmax*

Introduction

In recent years, positron emission tomography (PET), particularly with [18F] fluorodeoxyglucose (FDG), has emerged an alternative to computed tomography (CT) not only in treatment evaluation [1,2] but also in the staging of malignant lymphomas [3–6] even in cases of bone marrow involvement [7]. It enables the assessment of the extent of lymphoma with a higher sensitivity than that of CT [3–5,7].

In non-Hodgkin lymphoma (NHL), the Ki-67 proliferating index (MIB-1 labeling index) indicates the proliferation potential of tumor cells, which often affects the prognosis [8–10]. Although the correlation between the standardized uptake value (SUV) on PET and the proliferation potential of tumor cells has been reported in several tumors such as brain tumors [11], head and neck cancer [12], lung cancer [13], and bone and soft tissue tumors [14], it has barely been elucidated in the case of malignant lymphoma, which is one of the tumors that is most sensitive to chemotherapy/radiotherapy. Previous reports have described methods of distinguishing between indolent histology NHL and aggressive histology NHL [15–19]. However, it is important to know the proliferation potential and, in turn, determine the speed of tumor growth to decide the appropriate regimen of initial chemotherapy. In this study, we attempted to clarify the correlation between maximum SUV (SUVmax) at the biopsy site

Correspondence: Naoto Tomita, MD, Department of Internal Medicine and Clinical Immunology, Yokohama City University Graduate School of Medicine, 3-9, Fukuura, Kanazawa-ku, Yokohama 236-0004, Japan. Tel: +81-45-787-2800. Fax: +81-45-786-3444. E-mail: cavalier@ch-yamate.dlenet.com

ISSN 1042-8194 print/ISSN 1029-2403 online © 2009 Informa Healthcare USA, Inc.
DOI: 10.3109/10428190903440953

and the tumor proliferation potential using the MIB-1 labeling index in the cases of NHL, along with the cases of Hodgkin lymphoma (HL).

Materials and methods

Patients

Of 200 consecutive patients with malignant lymphoma in Yokohama City University Hospital during the period February 2001 through October 2007, 53 patients were staged by PET or PET/CT. In seven of them, pathologically evaluable specimens could not be prepared, and in other five cases, the pathological diagnosis was composite lymphoma. The remaining 41 patients (36 NHL and 5 HL) were the subjects of this study. The SUVmax on PET or PET/CT at the biopsy site was evaluated. The decision of the biopsy site was dependent on each attending physician. PET or PET/CT was not necessarily performed before the biopsy. The biopsy was not always performed at the site showing the maximum SUVmax in the whole body.

The biopsied specimens were reviewed by a hematopathologist (KT) according to the WHO classification [20], and the proliferation potential of lymphoma cells was evaluated by two pathologists (SS and KT) by measuring the MIB-1 labeling index in tumor cells. After evaluating the approximate proportion and distribution of lymphoma cells on the preparation stained by hematoxylin and eosin or immunostaining such as CD20, the MIB-1 labeling index was measured by Ki-67 immunostaining on the seriate section. The MIB-1 labeling index was measured by semiquantitative analysis and categorized into seven levels on the basis of the MIB-1 labeling grade (MG); MG-1 (nearly 0%), MG-2 (5–20%), MG-3 (21–40%), MG-4 (41–60%), MG-5 (61–80%), MG-6 (81–95%), and MG-7 (nearly 100%), respectively. The correlation between SUVmax at the biopsy site and the MIB-1 labeling index was analyzed in NHL. It was also compared between the cases biopsied from lymph nodes (LNs) and the cases done from extranodal (EN) sites. Furthermore, correlation was also analyzed for the subgroup of DLBCL. This study was approved by the ethical committee of Yokohama City University Hospital.

PET study

Studies were performed with the dedicated full ring PET (SET2400, Shimadzu, Kyoto, Japan) or LSO-based whole-body PET/CT scanner (Aquiduo, Toshiba Medical Systems, Tokyo, Japan). PET images were acquired with the following condition: field of view (FOV), 59.5 cm; body axis length, 20 cm; slice thickness, 3.125 mm; central resolution, 4.2 mm; and half width, 5.0 mm. The CT component of the PET/CT scanner was same as Aquillion 16, which has 16-rows detector. The PET component of the PET/CT scanner has a transaxial FOV of 68.3 cm and an axial FOV of 16.2 cm without septa and rotating rod source. The scanner was used in a three-dimensional mode with image resolution of 4.0 mm in full width at half maximum (FWHM). Before the PET/CT study, the patients fasted for at least 6 h. CT was performed from the head to the midthigh according to a standardized protocol with the following setting: axial 2.0-mm collimation × 16 modes; 120 kVp; Auto-Exposure Control (SD10); and a 0.5-s tube rotation, a table speed of 11.0 mm/s. Patients maintained normal shallow respiration during the acquisition of CT scans. No iodinated contrast material was administered. Emission scans from the head to the midthigh were obtained starting approximately 60 min adjusted for time decay until start of scan after the intravenous administration of 296–414 MBq of [18]F-FDG. The acquisition time for each PET was 2 min per table position. Images were reconstructed with attenuation-corrected, ordered-subset expectation maximization with two iterations and two subsets for dedicated PET or four iterations and 14 subsets using emission scans and CT data for PET/CT.

The initial review of the attenuation-corrected PET images was performed using transverse, coronal, and sagittal planes. The images were reviewed, and a diagnostic consensus was reached by two board-certified radiologists who were unaware of any clinical or radiologic information using a multimodality computer platform. Focal FDG uptake was considered to be abnormal when it was substantially greater than that of the surrounding normal tissue. A pixel region of interest (ROI) was outlined in the peak activity within regions of increased FDG uptake and measured on each slice. For quantitative interpretations, SUVmax was determined according to the standard formula, with activity in the ROI given in Bq per milliliter/injected dose in Bq per weight (kg). However, time decay correction for whole-body image acquisition was not conducted.

Statistical analysis

Mann–Whitney's test was used to calculate the differences between groups. Pearson's product moment correlation coefficient was used to calculate the correlations between SUVmax in the biopsy sites and the MIB-1 labeling index. The regression line has been depicted.

Results

There were eight indolent lymphoma cases, 26 aggressive lymphoma cases, two mantle-cell lymphoma cases, and five HL cases. The indolent lymphoma cases included three cases of follicular lymphoma (grade 1), and five cases of EN marginal zone lymphoma of mucosa-associated lymphoid tissue. Aggressive lymphoma cases included one case of T lymphoblastic lymphoma; 16 diffuse large B-cell lymphoma, not otherwise specified (DLBCL, NOS); one anaplastic lymphoma kinase (ALK)-positive large B-cell lymphoma; one plasmablastic lymphoma; one Burkitt lymphoma; one NK/T cell lymphoma, nasal type; one peripheral T-cell lymphoma, NOS; two angioimmunoblastic T-cell lymphoma; one anaplastic large-cell lymphoma, ALK positive; and one anaplastic large-cell lymphoma, ALK negative. All of the five cases with HL were nodular sclerosis subtype. HIV status was negative in all the 30 tested cases, including one case of plasmablastic lymphoma.

In NHL, the SUVmax at the biopsy sites ranged from 1.1 to 32.8 (Table I). It was significantly higher in the aggressive lymphoma cases than in the indolent lymphoma cases ($P < 0.001$). All eight cases with indolent lymphoma as well as the mantle-cell lymphoma cases exhibited a SUVmax below eight. On the other hand, only 23% (6 of 26) of aggressive lymphoma cases exhibited a SUVmax below eight. With regard to the MIB-1 labeling index, there were seven MG-1 cases, three MG-2 cases, three MG-3 cases, six MG-4 cases, 11 MG-5 cases, two MG-6 cases, and four MG-7 cases. The MIB-1 labeling index of the eight indolent NHL cases was significantly lower than that of the 26 aggressive NHL cases ($P < 0.001$). A strong positive correlation was observed between SUVmax at the biopsy sites and the MIB-1 labeling index in the 36 patients (Figure 1(a), $r = 0.69$, $P < 0.001$). The mathematical expression of the regression line was as follows: MIB-1 labeling index (%)$= 17.32 + 2.84$ SUVmax ($P < 0.001$, $R^2 = 0.47$).

Table I. SUVmax in biopsy site and MIB-1 index in NHL.

	n	SUVmax	MIB-1 index* (%)
Total	36	9.1 (1.1–32.8)	50 (0–100)
Indolent lymphoma	8	4.0 (1.1–7.1)	0 (0–10)
Aggressive lymphoma	26	11.7 (2.1–32.8)	70 (10–100)
Mantle-cell lymphoma	2	3.5 (2.1–4.9)	20 (10–30)
LN	19	9.1 (1.1–32.8)	50 (0–100)
EN	17	9.2 (1.3–22.5)	50 (0–100)

LN, lymph node; EN, extranodal site.
*Median (range).

All 15 cases with a SUVmax more than 10 exhibited an MG ≥ 4. Nineteen LN and 17 EN sites were biopsied. The EN sites were: tonsils–three cases; pharynx–two cases; bone–two cases; lung–two cases; orbita–one case; paranasal sinus–one case; salivary glands–one case; lip–one case; gingival–one case; stomach–one case; small intestine–one case; and prostate–one case. The SUVmax and MIB-1 labeling index were not significantly different between the LN and EN groups. A positive correlation was also observed between SUVmax at the biopsy sites and the MIB-1 labeling index in LN group ($r = 0.60$, $P = 0.006$) and EN group ($r = 0.87$, $P < 0.001$), respectively [Figure 1(b)]. In DLBCL only, a positive correlation was also observed ($r = 0.61$, $P = 0.01$) (data not shown). Samples of three cases with DLBCL, NOS indicating the positive correlation between SUVmax at the biopsy site, and the MIB-1 labeling index are shown in Figure 2. In HL, the SUVmax at the biopsy sites

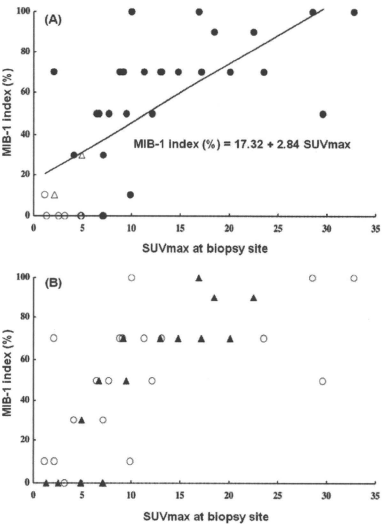

Figure 1. (a) There is a positive correlation between the SUVmax at biopsy site and MIB-1 labeling index in 36 cases of NHL ($r = 0.69$, $P < 0.001$). Regression line is depicted (○, indolent lymphoma; ●, aggressive lymphoma; △, mantle-cell lymphoma); (b) There are positive correlations between the SUVmax at biopsy site and MIB-1 labeling index in LN cases (○; $n = 19$, $r = 0.60$, $P = 0.006$) and in EN cases (▲; $n = 17$, $r = 0.87$, $P < 0.001$), respectively.

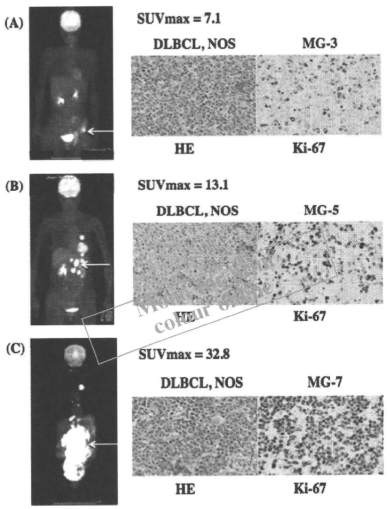

Figure 2. Samples showing the correlation between SUVmax at the biopsy site and the MIB-1 labeling grade (MG). (a) Left inguinal lymph node biopsy (SUVmax 7.1 and MG-3); (b) mesenteric lymph node biopsy (SUVmax 13.1 and MG-5); and (c) retroperitoneal lymph node biopsy (SUVmax 32.8 and MG-7).

ranged from 1.9 to 17.2 (median, 10.1). Almost all of the tumor cells were positive for Ki-67 staining and all of them were categorized in MG-7.

Discussion

The result of this study indicates that it is possible to estimate the proliferation potential from SUVmax on FDG-PET. It demonstrates the speed of tumor growth more directly and objectively compared with several previous reports [15–19] that indicate that SUVmax can be used as a predictor to distinguish between indolent histology and aggressive histology NHL cases. Therefore, our results have increased the importance of the SUV value on PET in the case of NHL. We can also estimate the proliferation potential of tumors in cases where the diagnostic biopsy is performed at sites other than the site of maximum SUVmax in the whole body or when PET is possible, but rebiopsy is clinically impossible in relapsed cases. The positive correlation between the SUVmax in biopsied site and the MIB-1 labeling index was stronger in EN group than in LN group, although the reason was uncertain.

In addition, we examined five cases with HL of the nodular sclerosis subtype during this period. Almost all the Hodgkin and Reed-Sternberg (HRS) cells were stained with MIB-1. The high MIB-1 labeling index of HRS cells, however, does not reflect the clinical behavior of the HL. Such a small number limits any meaning analysis. We excluded the HL cases in discussing the correlation between SUVmax and MIB-1 labeling index, all of which were MG-7.

Although our findings suggest an important role of SUVmax on PET in NHL, there are limitations to the use of SUVmax in the management of patients with NHL. In our study, 23% of aggressive lymphomas had SUVmax below eight, whereas all indolent lymphoma had SUVmax less than eight. There was still a considerable overlap between indolent and aggressive lymphoma. It suggests that SUVmax cannot completely distinguish between indolent and aggressive lymphoma. A positive correlation was observed between the SUVmax on FDG-PET at the biopsy site and the MIB-1 labeling index in NHL. The SUVmax is an useful predictor of the proliferation potential in NHL.

Declaration of interest: The authors report no conflicts of interest. The authors alone are responsible for the content and writing of the paper. ①

References

1. Juweid ME, Stroobants S, Hoekstra OS, et al. Use of positron emission tomography for response assessment of lymphoma: consensus of the Imaging Subcommittee of International Harmonization Project in Lymphoma. J Clin Oncol 2007;25: 571–578.
2. Cheson BD, Pfistner B, Juweid ME, et al. Revised response criteria for malignant lymphoma. J Clin Oncol 2007;25:579–586.
3. Hoh CK, Glaspy J, Rosen P, et al. Whole-body FDG-PET imaging for staging of Hodgkin's disease and lymphoma. J Nucl Med 1997;38:343–348.
4. Jerusalem G, Beguin Y, Najjar F, et al. Positron emission tomography (PET) with 18F-fluorodeoxyglucose (18F-FDG) for the staging of low-grade non-Hodgkin's lymphoma (NHL). Ann Oncol 2001;12:825–830.
5. Schöder H, Meta J, Yap C, et al. Effect of whole-body (18) F-FDG PET imaging on clinical staging andmanagement of patients with malignant lymphoma. J Nucl Med 2001;42:1139–1143.
6. Kwee TC, Kwee RM, Nievelstein RA. Imaging in staging of malignant lymphoma: a systematic review. Blood 2008;111: 504–516.
7. Moog F, Bangerter M, Kotzerke J, Guhlmann A, Frickhofen N, Reske SN. 18-F-fluorodeoxyglucose-positron emission tomography as a new approach to detect lymphomatous bone marrow. J Clin Oncol 1998;16:603–609.
8. Szczuraszek K, Mazur G, Jeleń M, Dziegiel P, Surowiak P, Zabel M. Prognostic significance of Ki-67 antigen expression in non-Hodgkin's lymphomas. Anticancer Res 2008;28:1113–1138.